Smectic-B phase and temperature-driven smectic-B to -A transition in concentrated solutions of "gapped" DNA

Prabesh Gyawali,[1] Rony Saha,[1] P. M. Sineth G. Kodikara,[1] Ruipeng Li,[2] Masafumi Fukuto,[2] James T. Gleeson,[1] Gregory P. Smith,[3] Noel A. Clark,[3] Antal Jakli,[1,*] Hamza Balci,[1] and Samuel Sprunt[1,†]

[1] *Department of Physics, Kent State University, Kent, OH 44242*
[2] *National Synchrotron Light Source II, Brookhaven National Laboratory, Upton, NY 11973*
[3] *Department of Physics, University of Colorado, Boulder, CO 80309*

(Dated: January 27, 2022)

The occurrence of a smectic-B phase is demonstrated in concentrated aqueous solutions of "gapped" DNA constructs consisting of fully-paired duplexes bridged by a flexible, unpaired strand of nucleotides. The B phase, identified by small and wide angle X-ray scattering measurements and optical microscopy, develops from a smectic-A phase with increasing DNA concentration at room temperature. It transitions (reversibly) to the smectic-A when the temperature is raised to $\sim 60^{\circ}$C.

I. INTRODUCTION

In recent years, studies on mesophasic self-assembly in aqueous solutions of ultra-short DNA duplexes or their oligomeric precursors [1–4], together with investigations of elementary lamellar (smectic-A) ordering of "gapped" DNA (duplexes bridged by a single strand of unpaired nucleotides) [5, 6] and of fully-paired duplexes capped at one end by a short hairpin [7], have reinvigorated research into the liquid crystalline (LC) properties of the molecule of life. Building upon classic work on cholesteric and columnar LC phases in solutions of duplex DNA [8–12], the new developments point to richer mesomorphic behavior that is achievable by simple manipulations of the morphology of individual DNA constructs.

The smectic-A (Sm A) phase of aqueously dispersed "gapped" DNA (GDNA) occurs in the concentration range $c_{DNA} \sim 230-260$ mg/ml, largely at the expense of the cholesteric state. It exhibits a significant sensitivity to temperature and, depending on the length of the gap, features either a mono- or bilayer structure (~ 1 or 2 duplex layer spacing, respectively) [6]. The smectic ordering and its temperature dependence were attributed to a combination of enthalpic interactions and entropic effects: Hydrophobic attraction between blunt duplex ends favors end-to-end stacking of the duplex segments between GDNA constructs, while segregation of the flexible single-strand "gaps" into layers becomes entropically favorable when the constructs are densely packed.

The present work addresses the questions: What happens to the Sm A phase in GDNA, and what role does temperature play, at higher DNA density? When concentrated above the cholesteric state, fully-paired duplexes transition to a 2D hexagonal columnar phase at $c_{DNA} \sim 400$ mg/ml and then, at $\sim 500-700$ mg/ml, they form 3D hexagonal and orthorhombic crystals [11, 12]. Here we demonstrate that LC solutions of GDNA constructs transform to a higher order smectic phase, which we identify as a lyotropic smectic-B (Sm B) phase, at substantially lower concentrations ($260-290$ mg/ml), and undergo a thermotropic transition to the Sm A phase in the $\sim 55-60^{\circ}$C temperature range. Our results further expose the distinct and remarkably rich LC properties of DNA constructs that incorporate rigid and flexible elements. They are also compelling since Sm B phases appear to be relatively rare in lyotropic systems: To our knowledge, prior reports are limited to colloidal suspensions of charged, inorganic platelet- [13] or rod- [14] shaped particles, and dense solutions of semi-flexible rodlike viruses [15–17].

II. EXPERIMENTAL DETAILS

The investigated GDNA construct, denoted 48-10T-48, consists of two, symmetric 48 bp duplexes connected by a single-strand "gap" of 10 unpaired thymine bases (Fig. 1). The construct was synthesized from PAGE-purified oligomers purchased from ExonanoRNA (Columbus, OH, USA). Details of the synthesis and the specific nucleotide sequences are described elsewhere [6].

For small/wide-angle x-ray scattering (SAXS/WAXS) studies, we prepared dense aqueous solutions of 48-10T-48 constructs in standard borosilicate capillaries with 1.25 mm inner diameter as follows: We first slowly and evenly loaded a ~ 40 μL volume of isotropic solution ($c_{DNA} \sim 80-100$ mg/ml) into an open capillary, and then very gradually allowed the water component of the buffer to evaporate until a target volume was reached. The components of the initial buffer solution were adjusted so that after the water evaporation, the buffer composition was approximately 150mM NaCl/10mM Tris/0.1 mM thylenediaminetetraacetic acid (EDTA) in deionized water at pH 7.5. From the known c_{DNA} of the initial solution and the known sample volume after evaporation, the final c_{DNA} could be estimated to an accuracy of $\pm 5\%$. The capillaries were sealed when the DNA concentration was in the range $c_{DNA} = 260-290$ mg/ml –

* Advanced Materials and Liquid Crystals Institute, Kent State University, Kent, OH 44242
† ssprunt@kent.edu; Advanced Materials and Liquid Crystals Institute, Kent State University, Kent, OH 44242

$\sim$ 10 mg/ml above the range of the Sm A phase previously investigated [6] – and then stored at 4°C for several weeks prior to study.

Polarizing optical microscopy (POM) was performed on samples sandwiched between 1 mm thick microscope slides. The samples were sealed by a thin ring of mineral oil after water had evaporated from the edges of the film to the point where focal conic (FC) textures appeared, signaling the development of a smectic phase. To confirm that the orientation of the GDNA duplex segments in the FCs is consistent with a smectic layer structure, we utilized a wedge-shaped quartz compensator plate that could be inserted into the optical path between crossed polarizer and analyzer, at a 45° angle to the polarizer axis. By sliding the plate a variable distance into the optical path, the phase shift between light polarized parallel and perpendicular to the optic axis of the plate could be varied. The variable retardation, combined with the birefringence and dispersion of the GDNA sample, enables one to determine the orientation of the optic axis in the FC domains by referencing the color of light transmitted through the sample to a Michel-Levy interference color chart [18].

SAXS/WAXS measurements were carried out on beamline 11-BM at the National Synchrotron Light Source II. The incident x-ray energy was 17 keV, the incident beam size at the sample was 0.2×0.2 mm, and the SAXS area detector was positioned 3 m from the sample. No evidence of x-ray damage to samples was observed during the $10 - 30$ s data acquisition times. Samples were mounted in a modified commercial hot/cold stage (Instec HCS60) with kapton film windows. The temperature of the sample was regulated between 5° and 65°C (safely below the 77°C denaturation temperature of the 48 bp GDNA duplexes).

III. RESULTS

A. Optical microscopy

Smectic layering in GDNA samples is revealed in the polarizing microscope by a focal conic "fan" texture in which the duplexes orient radially away from the core of individual FCs. As described in the Experimental section, the orientation may be deduced using an optical compensation plate. In order to minimize the cost in elastic energy (i.e., preserve approximately uniform layer spacing), the smectic layers of GDNA bend azimuthally around the FC core, and there is a corresponding splay in the duplex orientation. (By contrast, fully-paired duplexes in the columnar phase orient azimuthally within similar-appearing FC domains [3], and thus undergo an orientational bend in these domains).

Fig. 1 shows two variants of the fan texture coexisting at 25°C in a thin film of 48-10T-48 sandwiched between glass slides and sealed as described above. The DNA concentration increases from left to right. The dashed yellow line tracks a boundary between smooth (lower c_{DNA}) and striated (higher c_{DNA}) fan textures to the left and right of the line, respectively. The four images at the bottom of Fig. 1 show details of striated FCs with different "fan" orientations, before and after the compensator plate was inserted. (Its optical axis is labeled $\hat{e}$ in the figure.) After the compensator is inserted, the color shifts (relative to background color) observed between "fans" oriented along and perpendicular to $\hat{e}$, together with the negative optical anisotropy of DNA duplexes [19–21], confirm a radial duplex orientation within the FCs.

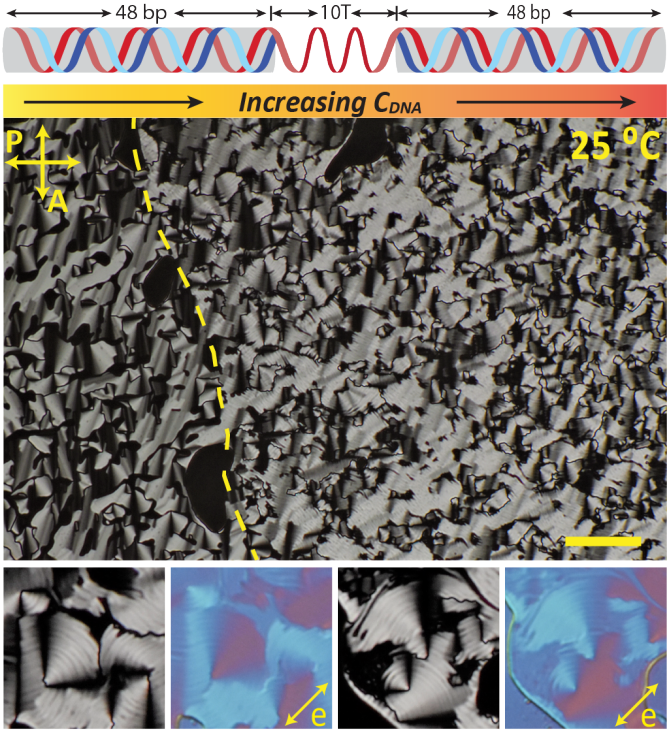

FIG. 1: *Top:* Schematic structure of the 48-10T-48 GDNA construct studied. *Middle image*: Polarizing optical microscopy of smectic focal conic (FC) "fan" textures in a thin film of 48-10T-48 GDNA solution sandwiched between glass slides at 25°C. The dashed yellow line separates distinct "smooth" and "striated" FC textures (to the left and right of the line, respectively) that are observed in the presence of a positive DNA concentration gradient running from left to right. Scale bar = 50μm. *Bottom images:* Detail of striated FC domains with (images in color) and without (black/white) a quartz compensator inserted in the optical path. Relative color shifts observed in radial directions from the "tip" of an isolated FC that are along and normal to the compensator's optical axis (labeled e) indicate radial orientation of the GDNA duplexes. This is consistent with smectic layers that bend along the azimuthal direction in the FC.

We previously used the same technique to associate the smooth fan texture with the Sm A phase in GDNA [6].

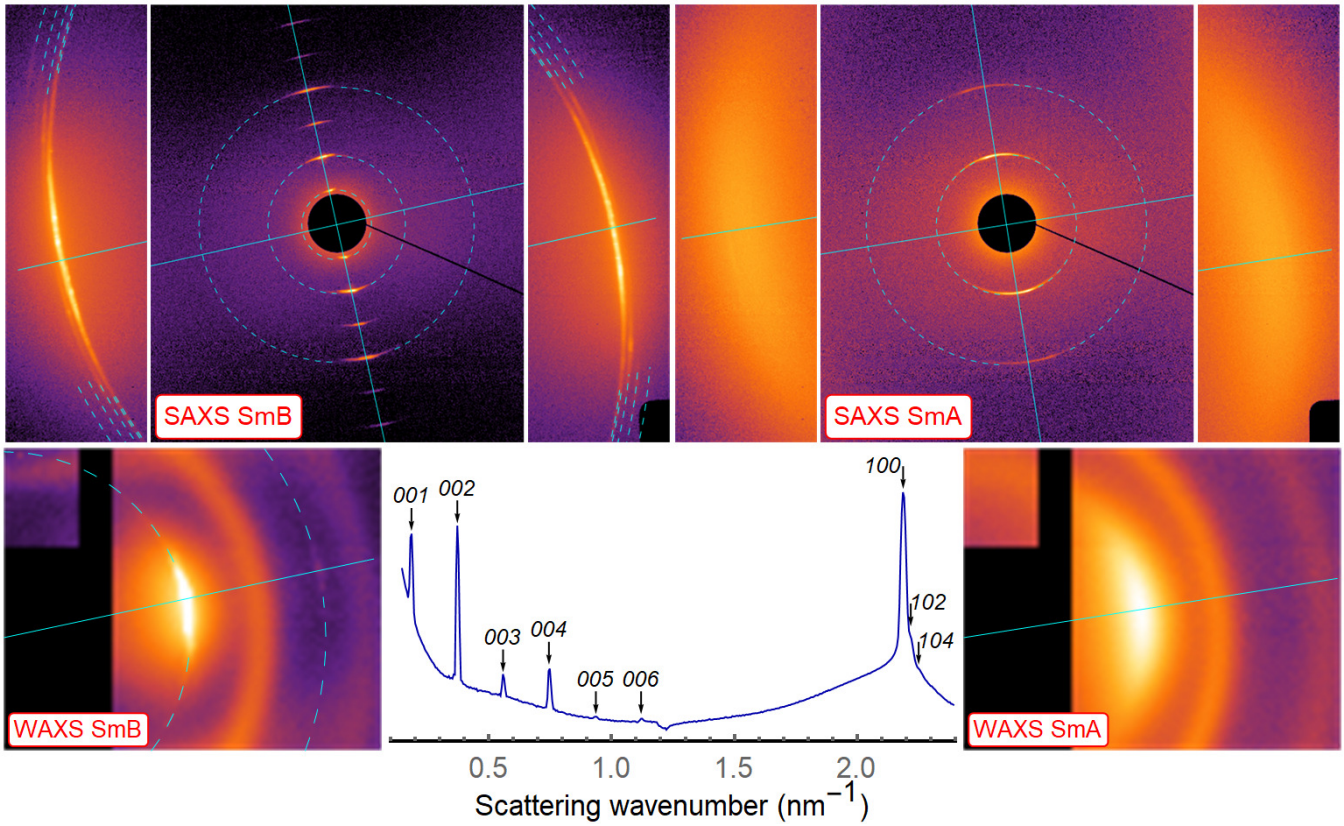

FIG. 2: *Top left and right:* 2D SAXS patterns recorded on oriented domains of a 265 mg/ml 48-10T-48 sample in the Sm B phase at 15.3°C (left) and Sm A phase at 52.8°C (right). The central image in each case shows the small angle diffraction arising from layering of the duplex segments ($00l$ peaks, with the $l = 1, 2, 4$ orders indicated with dashed blue circles for reference). The left and right side images are blow-ups of the wider angle scattering due to the lateral packing of the duplexes within the layers. In the Sm B phase, this scattering consists of narrowly spaced, sharp arcs, indicated by the blue dashed lines, which index as $10l$ ($l = 0$ dominating, with much weaker features for $l = 2, 3, 4$ being just visible). In the Sm A phase, the arcs are replaced by diffuse scattering. *Bottom left and right:* 2D WAXS patterns recorded in the Sm B and Sm A phases simultaneously with the SAXS patterns. In the Sm B phase (bottom left), the dashed blue arcs indicate 100 and (much weaker) 110 peaks indexed for a 2D hexagonal lattice. *Bottom middle:* Log of azimuthally-averaged X-ray intensity vs q obtained from the SAXS pattern at top left (Sm B phase), with six $00l$ and three resolvable $10l$ reflections labeled. The SAXS and WAXS patterns are rendered after the log of the pixel values was taken (with a small offset). The diffuse ring in the WAXS images just beyond the 100 peak is scattering from kapton windows.

As water evaporates from the sample edge, the smooth texture appears first and then evolves after further evaporation to the striated texture, which migrates inward from the edge. It is therefore reasonable to attribute the striated texture, developing at higher DNA concentration than the Sm A, to a distinct, higher order smectic phase. In small molecule thermotropic LCs, a similar texture signals a Sm A to smectic-B (Sm B) phase transition in cooling [22], although the stripes decorating the FC fans rapidly fade with time as the Sm B order equilibrates thermally. In the GDNA system, the striped texture develops under gradients in c_{DNA}; the transitory nature of the striations is difficult to judge in this case, because any particular region of the sample is generally not in equilibrium with the neighboring regions.

To confirm the nature of the higher order phase in GDNA and to explore its temperature dependence, we turn to the results of SAXS/WAXS measurements.

B. Small and wide angle x-ray scattering

Fig. 2 shows representative 2D SAXS/WAXS patterns from fairly well oriented smectic domains (with layer normal nearly parallel to the detector plane) in a 265 mg/ml 48-10T-48 sample at temperatures $T = 15.3$ and 52.8°C. At the lower temperature, six orders of diffraction are recorded at small angles (Fig. 2, top left). The lowest order (at scattering wavenumber $q = 0.187$ nm^{-1}) corresponds to a spatial periodicity of $d = 2\pi/q = 33.6$ nm,

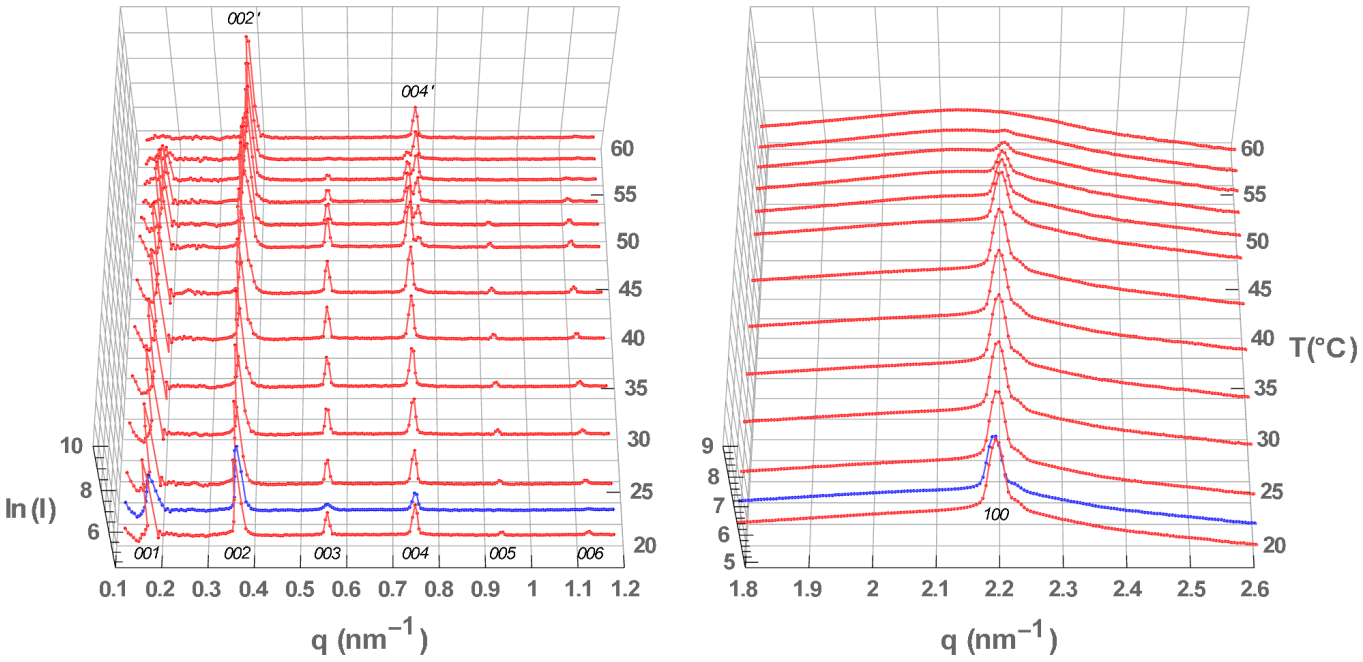

FIG. 3: Temperature dependence of the log of the azimuthally-averaged SAXS intensity from a 285 mg/ml 48-10T-48 GDNA sample. The left panel shows the diffraction from the smectic layer structure with peaks indexed as $00l$ in the Sm B phase and $00l'$ in the Sm A phase, and the right panel shows a detail of 100 peak diminishing with increasing temperature. Traces in red correspond to heating from the Sm B to A phase, and the traces in blue are obtained after subsequent cooling back to the Sm B.

slightly greater than two duplex lengths. We index the peaks as $00l$ with corresponding scattering vector $\vec{q}_{00l}$ along the layer normal. Their number and full width at half maximum (FWHM) indicate domains with well-defined layer structure of average length at least 30 duplexes along the layer normal. The alternating heights of the odd and even order peaks (Fig. 2, bottom middle) suggest a combination of mono- and bilayer components, with layer spacing $d/2$ and d, respectively, contribute to the overall smectic density wave.

At wider angles on the SAXS detector, intense scattering, centered azimuthally about the direction orthogonal to the smectic layer normal, is recorded at $q = 2.19$ nm^{-1} for the lower temperature (top left in Fig. 2). The sharpness of the peak and its orientation indicate significant positional correlations of the duplexes within the smectic layers. Weaker reflections, at 2.22, 2.26, and 2.31 nm^{-1} (narrowly spaced from the main peak and indicated by blue dashes in Fig. 2), are also visible. Additionally, as shown in Fig. 2 (bottom left), a very weak peak, also centered on the axis perpendicular to the layering direction, is recorded on the WAXS detector at $q = 3.79$ nm^{-1}. The ratio of wavenumbers for the intense and weak WAXS peaks, $3.79/2.19 = 1.73$, matches the expected relation between the 110 and 100 reflections from a hexagonal crystal structure, $q_{110}/q_{100} = \sqrt{3}$. Based on these assignments, we may index the weaker satellite reflections at 2.22, 2.26, and 2.31 nm^{-1} as $10l$ for $l = 2, 3, 4$, since they satisfy the relation $q_{10l} = \sqrt{q_{100}^2 + q_{00l}^2} = \sqrt{2.19^2 + (l \times 0.187)^2}$. As indicated by nearly overlapping blue dashed lines in Fig. 2 (top left), the peak "expected" at $q_{101} = 2.20$ nm^{-1} is too close to the intense scattering at $q_{100} = 2.19$ nm^{-1} to be resolved.

Based on the analysis and assignments above, we identify the lower temperature smectic phase as a Sm B phase, with layers of hexagonally-packed 48 bp duplex segments of the GDNA constructs stacked so that their blunt ends are paired, producing a ~ 2 duplex periodicity along the stacking direction. The lateral duplex-duplex spacing is $a = 4\pi/(\sqrt{3}q_{100}) = 3.31$ nm (center to center), and the typical lateral size of a monodomain (estimated from the FWHM of the 100 peak) is $\gtrsim 25a$.

The Sm B state of GDNA is strongly sensitive to temperature as well as concentration. At elevated temperatures, it melts reversibly into a Sm A phase. In particular, during heating from room temperature, the intense 100 scattering diminishes continuously and, together with the weak 110 peak, disappears completely between 50° and 60°C, leaving only diffuse scattering from the lateral packing of the duplexes consistent with fluid smectic layers (Fig. 2, top right). At the same temperature, the $00l$ peaks for odd l (associated with ∼two duplex periodicity)) also vanish, resulting in a Sm A phase with ∼single duplex layer spacing.

Detailed SAXS data vs temperature reveal a temperature range over which the Sm B phase coexists with the

Sm A phase. Fig. 3 (left panel) shows azimuthally averaged profiles of x-ray diffraction at small angles and various T from the smectic layer structure of a 48-10T-48 sample with c_{DNA} = 285 mg/ml. At $T \approx 43°$C, a secondary peak emerges at a q value just above the 002 peak associated with the low temperature (Sm B) layer structure. This new peak (designated $002'$) and its weaker harmonics ($004'$ and $006'$, the latter barely visible in Fig. 3) grow in amplitude as the scattering from Sm B domains diminishes, and eventually (at $T \approx 59°$C) account for all the observed small-angle scattering. Fig. 3 (right panel) shows the simultaneous diminution of the wider angle 100 peak on heating through the same temperature steps, and its replacement with a broad, diffuse peak. Thus, on heating to 59°C, the Sm B phase in the 285 mg/ml sample completely transforms to a Sm A state, with layer spacing $d' = 2\pi/q_{002'} = 16.6$ nm comparable to a single duplex length. When the sample is subsequently cooled back to 22°C, the Sm B phase reforms with the $00l$ ($l = 1-6$) and 100 peaks reappearing at their original positions (Fig. 3, blue traces), although the amplitudes do not fully recover over a 1 h period after cooling.

The Sm B to A transition occurs at a $\sim 7°$C higher temperature in the 285 mg/ml sample than in the more dilute (265 mg/ml) sample studied in Fig. 2. The dependence of the transition temperature on c_{DNA} appears to be significant, but so far we have not explored it in detail.

IV. DISCUSSION

In addition to hexagonal lateral packing of the duplexes, a model of the smectic-B phase in GDNA must account for both mono- and bilayer correlations, as evidenced by the presence of odd and even $00l$ orders of diffraction that alternate systematically in intensity, and by the disappearance of the odd orders at the Sm B to A transition (Figs. 2 and 3).

Fig. 4 presents schemes for the GDNA packing in the two phases that satisfy these requirements. The main idea is that the Sm B phase forms from a lower concentration (or higher temperature) Sm A phase in which the duplex segments from different GDNA constructs interdigitate within the smectic layers, and their blunt ends are generally separated. As suggested in Fig. 4, this arrangement allows the flexible single-strands in the "gap" segments to explore additional space laterally, while maintaining a relatively dense packing of duplexes in fluid monolayers (layer spacing comparable to a single duplex length). In this scenario, entropy prevails over enthalpic end-end interactions in minimizing the free energy.

At higher c_{DNA} (or lower temperature), the Sm B phase forms as the blunt ends of the duplex segments pair, and the duplexes pack side-by-side in a 2D hexagonal lattice. The attractive interaction between blunt ends – stronger at lower temperature and higher c_{DNA} (where the ends are more closely spaced) – reduces the free energy against a trade-off in entropy. The blunt end pairing eliminates lateral space available for the flexible "gap" segments to explore, and consequently forces their extension along the layer normal. This would account for the shift (Fig. 3) of the $002'$, $004'$, and $006'$ peaks in the Sm A phase to their positions at slightly lower q in the B phase.

As Fig. 4 shows, the development from purely monolayer to substantially bilayer correlations across the Sm A to B transition can be viewed as phase separation of a mixture of blunt duplex ends and "dressed" ends (i.e., ends connected to a flexible single strand) occupying planes parallel to the layers. The sequence from left to right in Fig. 4 shows an increasing degree of this separation, which accounts for the development of a pronounced bilayer (001) peak (and its odd-order harmonics) in the diffraction from the Sm B phase layer structure (Fig. 3). So far we have not observed the "limiting" case of complete separation of blunt and "dressed" duplex ends into consecutive planes (Fig. 4, right), which should produce monotonically decreasing intensity of the $00l$ reflections, in contrast to the alternating intensities for odd and even l in Fig. 3.

In the Sm B phase, pairing of the blunt ends and confinement of the single strands connecting the opposing (internal) ends imply a degree of interlayer coupling of the 2D hexagonal ordering. This could explain the weak $10l$ satellites to the 100 peak (Fig. 2, top left). On the other hand, the weak 110 scattering implies that the 2D hexagonal order within Sm B layers of GDNA is not as well developed as in the hexagonal crystalline phase of FDNA (which occurs at significantly higher c_{DNA}) [11].

Next consider the origin of the striated optical texture observed on FCs in smectic GDNA samples (Fig. 1). Below the Sm A to B transition the lateral spacing (a) between duplexes shrinks (compare centers of the diffuse Sm A and sharp Sm B peaks in Fig. 3, right), while the smectic layer spacing increases at the same time. Assuming this also happens when the transition occurs due to increasing c_{DNA} (at constant T), the lateral strain imposed by reduction in a could be relieved by a bend modulation in the duplex orientation along the layer normal, which is not inhibited by a fixed layer spacing because it is simultaneously changing. The accompanying modulation of the optical birefringence would then produce a stripe pattern, with the stripes parallel to the layers (i.e., running azimuthally across the "fan backs" in the optical texture). If the Sm B phase equilibrates slowly (due to slow water evaporation and slow relaxation of concentration gradients), the stripe pattern may persist for long times.

Finally, we should mention that we previously proposed [6] the model for the Sm A phase in Fig. 4 to account for the monolayer (∼single duplex) periodicity observed in smectic solutions of 48-nT-48 GDNA constructs with gap lengths $n \lesssim 10$. On the other hand, prior results on the Sm A phase of constructs with longer "gaps" ($n = 20$ in particular) indicated a purely bilayer

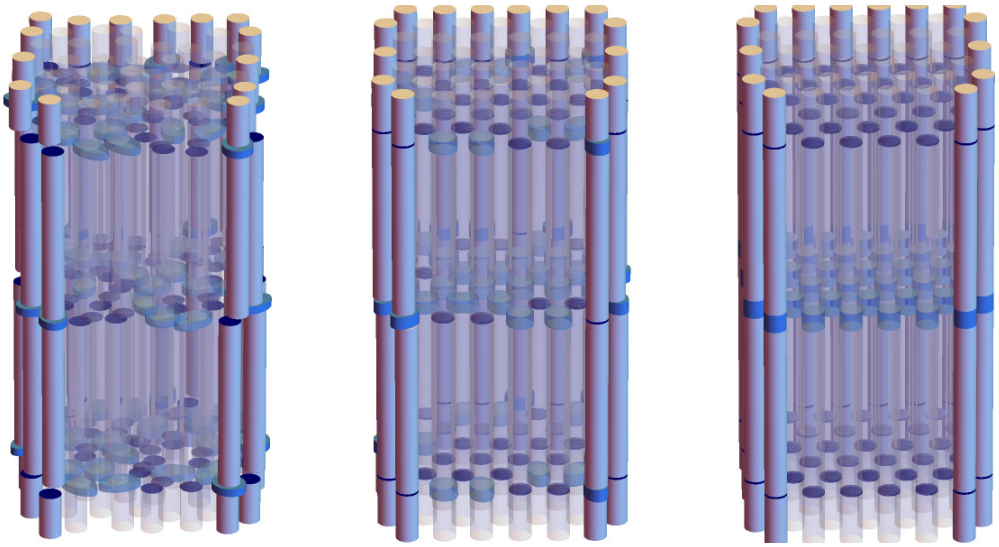

FIG. 4: Proposed schemes for GDNA packing in the smectic-A (left) and -B (middle and right) phases of 48-10T-48 GDNA solutions. On the left, right, and back sides of the domains shown, the duplexes are depicted as long, light-blue cylinders, the regions occupied by the single-strand "gap" segments are shown as short cylinders in a bolder blue, and the blunt duplex ends are highlighted in dark blue. Inside the domains, the constructs are rendered with transparency to reveal the interior arrangement. Partial layers of duplexes are shown at the top and bottom of the domain. *Left:* In the Sm A phase, the blunt duplex ends are separated, allowing the single-stranded segments to explore space and the duplexes to disorder within the layer planes. Interdigitation of duplexes from neighboring constructs results in a smectic density wave with ∼single duplex periodicity. *Middle:* Sm B phase with paired blunt ends and constructs stacked in vertical columns, which pack hexagonally in the lateral directions. Significant interdigitation persists; consequently, the small-angle diffraction is a superposition from density variations with ∼one and ∼two duplex periodicity, in agreement with the low temperature data in Fig. 3. *Right:* Sm B phase with full segregation of paired blunt duplex ends and single-stranded "gap" segments into alternating planes and enhanced 3D ordering. In this case, the small-angle diffraction profile should feature peaks at harmonics of $q \approx 2\pi/2d$ ($d \simeq$ duplex length) that decrease monotonically in intensity with q, which differs from the data in Fig. 3.

structure [5]. The present work, combined with these earlier studies, should motivate more detailed investigation of smectic phase morphology in solutions of GDNA with various "gap" lengths.

V. CONCLUSION

We have described a lyotropic smectic-B phase formed in solutions of "gapped" DNA duplexes with strong temperature dependence. Hexagonal in-layer order develops at room temperature when the DNA concentration increases above the range of the smectic-A phase previously discovered in this system, and a temperature-driven Sm B to Sm A transition occurs at fixed concentration when the sample is heated a few tens of degrees above room temperature. These results further support the conclusion that the phase diagram of DNA duplexes in the concentration range $\sim 200 - 300$ mg/ml, where liquid crystalline phases occur, shifts from exclusively cholesteric/columnar to predominantly layered (smectic) phases, when a sufficiently long segment of unpaired bases is introduced in the middle of an otherwise fully-paired construct. The flexible internal linkage and blunt end-end attractive interaction both play key roles in stabilizing the smectic phases and determining their remarkable combination of thermotropic and lyotropic behavior.

ACKNOWLEDGMENTS

The Kent State authors gratefully acknowledge support from the National Science Foundation under grant DMR-1904167. GPS and NAC were supported by the NSF under grant DMR-2005212. SAXS/WAXS measurements were conducted at the 11-BM CMS beamline of the National Synchrotron Light Source II, a U.S. Department of Energy (DOE) Office of Science User Facility operated for the DOE Office of Science by Brookhaven National Laboratory under Contract No. DE-SC0012704.

[1] M. Nakata, G. Zanchetta, B. D. Chapman, C. D. Jones, J. O. Cross, R. Pindak, T. Bellini, and N. A. Clark, *End-to-End Stacking and Liquid Crystal Condensation of 6–to 20–Base Pair DNA Duplexes*, Science **318**, 1276 (2007).

[2] T. Bellini, G. Zanchetta, T. P. Fraccia, R. Cerbino, E. Tsai, G. P. Smith, M. J. Moran, D. M. Walba, and N. A. Clark, *Liquid Crystal Self-Assembly of Random-Sequence DNA Oligomers*, Proc. Natl. Acad. Sci. U.S.A. **109**, 1110 (2012).

[3] T. P. Fraccia, G. P. Smith, L. Bethge, G. Zanchetta, G. Nava, M. J. Moran, S. Klussmann, N. A. Clark, and T. Bellini, *Liquid Crystal Ordering and Isotropic Gelation in Solutions of Four-Base-Long DNA Oligomers*, ACS Nano **10**, 8508 (2016).

[4] G. P. Smith, T. P. Fraccia, M. Todisco, G. Zanchetta, C. Zhu, E. Hayden, T. Bellini, and N. A. Clark, *Backbone-free duplex-stacked monomer nucleic acids exhibiting Watson–Crick selectivity*, Proc. Natl. Acad. Sci. U.S.A. **115**, E7658 (2018).

[5] M. Salamonczyk, J. Zhang, G. Portale, C. Zhu, E. Kentzinger, J. T. Gleeson, A. Jakli, C. D. Michele, J. K. G. Dhont, S. Sprunt, and E. Stiakakis, *Smectic phase in suspensions of gapped DNA duplexes*, Nat. Commun. **7**, 13358 (2016).

[6] P. Gyawali, R. Saha, G. P. Smith, M. Salamonczyk, P. Kharel, S. Basu, R. Li, M. Fukuto, J. T. Gleeson, N. A. Clark, A. Jakli, H. Balci, and S. Sprunt, *Mono- and bilayer smectic liquid crystal ordering in dense solutions of "gapped" DNA duplexes*, Proc. Natl. Acad. Sci. USA **118**, e2019996118 (2021).

[7] K. Gvozden, S. N. Ratajczak, A. G. Orellana, E. Kentzinger, U. Rücker, J. K. G. Dhont, C. D. Michele, and E. Stiakakis, *Self-Assembly of All-DNA Rods with Controlled Patchiness*, Small , DOI: 10.1002/smll.202104510 (2021).

[8] T. E. Strzelecka, M. W. Davidson, and R. L. Rill, *Multiple Liquid Crystal Phases of DNA at High Concentrations*, Nature **331**, 457 (1988).

[9] F. Livolant, A. M. Levelut, J. Doucet, and J. P. Benoit, *The Highly Concentrated Liquid-Crystalline Phase of DNA Is Columnar Hexagonal*, Nature **339**, 724 (1989).

[10] F. Livolant, *Ordered Phases of DNA in Vivo and in Vitro*, Physica A **176**, 117 (1991).

[11] D. Durand, J. Doucet, and F. Livolant, *A Study of the Structure of Highly Concentrated Phases of DNA by X-Ray Diffraction*, Journal de Physique II **2**, 1769 (1992).

[12] F. Livolant and A. Leforestier, *Condensed Phases of DNA: Structures and Phase Transitions*, Prog. Polym. Sci. **21**, 1115 (1996).

[13] D. Kleshchanok, P. Holmqvist, J.-M. Meijer, and H. N. W. Lekkerkerker, *Lyotropic Smectic B Phase Formed in Suspensions of Charged Colloidal Platelets*, J. Am. Chem. Soc. **134**, 5985 (2012).

[14] A. Kuijk, D. V. Byelov, A. V. Petukhov, A. van Blaaderena, and A. Imhofa, *Phase behavior of colloidal silica rods*, Faraday Discuss. **159**, 181 (2012).

[15] E. Grelet, *Hexagonal Order in Crystalline and Columnar Phases of Hard Rods*, Phys. Rev. Lett. **100**, 168301 (2008).

[16] E. Grelet, *Hard-Rod Behavior in Dense Mesophases of Semiflexible and Rigid Charged Viruses*, Phys. Rev. X **4**, 021053 (2014).

[17] A. Repula, M. O. Menegon, C. Wu, P. van der Schoot, and E. Grelet, *Directing Liquid Crystalline Self-Organization of Rodlike Particles through Tunable Attractive Single Tips*, Phys. Rev. Lett. **122**, 128008 (2019).

[18] W. Nesse, *Introduction to Optical Mineralogy*, 3rd ed. (Oxford University Press, New York, 2003).

[19] N. C. Stellwagen, *Electric birefringence of restriction enzyme fragments of DNA: optical factor and electric polarizability as a function of molecular weight*, Biopolymers **20**, 399 (1981).

[20] G. Maret and G. Weill, *Magnetic birefringence study of the electrostatic and intrinsic persistence length of DNA*, Biopolymers **22**, 2727 (1983).

[21] R. Oldenbourg and T. Ruiz, *Magnetic birefringence study of the electrostatic and intrinsic persistence length of DNA*, Biophys. J. **56**, 195 (1989).

[22] G. W. Gray and J. W. Goodby, *Smectic Liquid Crystals: Textures and Structures* (Leonard Hill, London, 1984).